ErbB4 tyrosine kinase inhibition impairs neuromuscular development in zebrafish embryos

Ilkka Paatero[a,b,c,d,e], Ville Veikkolainen[a,b], Matias Mäenpää[a], Etienne Schmelzer[c], Heinz-Georg Belting[c], Lauri J. Pelliniemi[a], and Klaus Elenius[a,b,f,*]

[a]Institute of Biomedicine, [b]Medicity Research Laboratory, [d]Laboratory of Animal Physiology, Department of Biology, and [f]Department of Oncology, University of Turku, FIN-20520 Turku, Finland; [c]Biozentrum der Universität Basel, CH-4056 Basel, Switzerland; [e]Turku Centre for Biotechnology, University of Turku and Åbo Akademi University, FIN-20520 Turku, Finland

ABSTRACT **Tyrosine kinase inhibitors are widely used in the clinic, but limited information is available about their toxicity in developing organisms. Here, we tested the effect of tyrosine kinase inhibitors targeting the ErbB receptors for their effects on developing zebrafish (*Danio rerio*) embryos. Embryos treated with wide-spectrum pan-ErbB inhibitors or *erbb4a*-targeting antisense oligonucleotides demonstrated reduced locomotion, reduced diameter of skeletal muscle fibers, and reduced expression of muscle-specific genes, as well as reduced motoneuron length. The phenotypes in the skeletal muscle, as well as the defect in motility, were rescued both by microinjection of human *ERBB4* mRNA and by transposon-mediated muscle-specific *ERBB4* overexpression. The role of ErbB4 in regulating motility was further controlled by targeted mutation of the endogenous *erbb4a* locus in the zebrafish genome by CRISPR/Cas9. These observations demonstrate a potential for the ErbB tyrosine kinase inhibitors to induce neuromuscular toxicity in a developing organism via a mechanism involving inhibition of ErbB4 function.**

Monitoring Editor
Marianne Bronner
California Institute of Technology

Received: Jul 30, 2018
Revised: Nov 1, 2018
Accepted: Nov 16, 2018

INTRODUCTION

Despite the approval of a number of molecularly targeted therapies for treating several different cancer types, only a few protocols have been clinically tested with pediatric patients. Drugs approved for treatment of malignancies in adults are still often used off-label for pediatric patients (Zwaan *et al.*, 2010). Clinical pharmacology of children, however, differs significantly from that of adults (Kearns *et al.*, 2003), and the developing organs may be expected to be more vulnerable to toxicity than their mature adult counterparts, with a higher percentage of slowly dividing or quiescent cells. In particular, this is of potential concern in the case of inhibitors of growth-signaling molecules, such as the receptor tyrosine kinases (RTK).

ErbB receptors are a subfamily of RTKs composed of four members: epidermal growth factor receptor (EGFR, ErbB1, HER1), ErbB2 (HER2), ErbB3 (HER3), and ErbB4 (HER4). ErbB1 and ErbB2 have been successfully targeted in different cancer types, such as breast, lung, colorectal, gastric, and head and neck, by both therapeutic antibodies and tyrosine kinase inhibitors (TKI; Arteaga and Engelman, 2014). The recently developed wide-spectrum ErbB TKIs, including afatinib, neratinib, canertinib, and dacomitinib, suppress the catalytic activity of EGFR and ErbB2 as well as ErbB4, while they do not directly target the naturally nearly kinase-inactive ErbB3 (Schwartz *et al.*, 2014).

During development, the ErbB receptors activate central signaling pathways that regulate vertebrate organogenesis (Holbro and Hynes, 2004). A typical mammalian genome includes four *erbb* genes, *erbb1*, *erbb2*, *erbb3*, and *erbb4* (Stein and Staros, 2000). In the zebrafish (*Danio rerio*) genome, however, the genes encoding EGFR, ErbB3, and ErbB4 have been suggested to have undergone another round of duplication, producing *erbb1a* and *erbb1b*, *erbb3a* and *erbb3b*, and *erbb4a* and *erbb4b*, while there is only a single *erbb2* gene (Reischauer *et al.*, 2009).

This article was published online ahead of print in MBoC in Press (http://www.molbiolcell.org/cgi/doi/10.1091/mbc.E18-07-0460) on November 21, 2018.

The authors declare that they have no conflicts of interest.

*Address correspondence to: Klaus Elenius (klaele@utu.fi).

Abbreviations used: AchR, acetylcholine receptor; CRISPR, clustered regularly interspaced short palindromic repeats; DAPI, 4′,6-diamidine-2-phenylindole; DMSO, dimethyl sulfoxide; EGFP, enhanced green fluorescent protein; erbb4, erb-b2 receptor tyrosine kinase 4; FPKM, fragments per kilobase of exon model per million reads mapped; hpf, hours postfertilization; HRP, horseradish peroxidase; HTA, head-trunk angle; PBS, phosphate-buffered saline; PFA, paraformaldehyde; RTK, receptor tyrosine kinase; RT-PCR, reverse transcription-PCR; sgRNA, single-guide RNA; TKI, tyrosine kinase inhibitor.

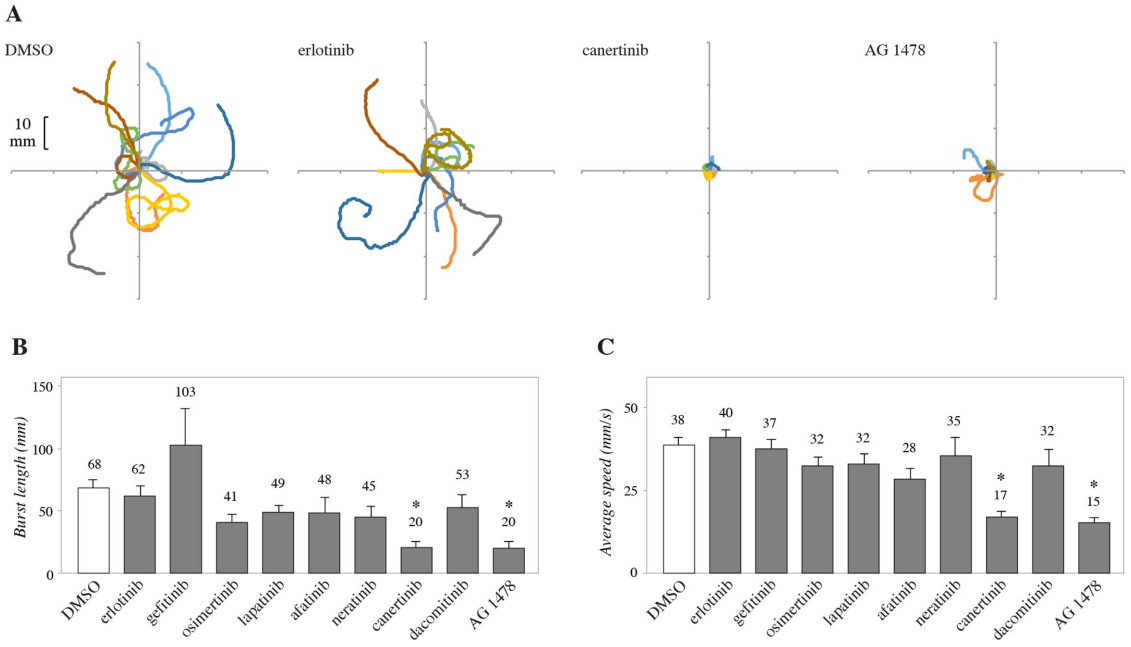

FIGURE 1: ErbB kinase inhibitors reduce motility of zebrafish embryos. Touch–response assays measuring motility of embryos treated from 8 to 48 hpf with the buffer control DMSO or with 10 μM of the indicated ErbB TKIs. (A) The colored lines demonstrate videorecorded tracks of swim bursts of individual embryos stimulated to move by a physical touch to the tail. (B, C) Quantification of the length of the entire swim burst (B) and the average speed during the burst (C) in the touch–response assays. Mean values are indicated above each column. DMSO, $n = 18$; erlotinib, $n = 14$; gefitinib, $n = 11$; osimertinib, $n = 9$; lapatinib, $n = 7$, afatinib, $n = 7$; neratinib, $n = 6$; canertinib, $n = 7$; dacomitinib, $n = 9$; AG 1478, $n = 11$. *$p < 0.05$.

One approach to preclinically addressing the toxicity of RTK TKIs is analyzing experimental models of growing organisms. Zebrafish embryos and larvae are an increasingly used model both for pediatric research (Veldman and Lin, 2008; Lohi *et al.*, 2013) and for in vivo testing of drug efficacy and toxicology (MacRae and Peterson, 2015). Here, we tested several ErbB-targeting TKIs for toxicity in zebrafish embryos. Our findings indicate that wide-spectrum pan-ErbB TKIs, but not EGFR-specific TKIs (nor TKIs with dual specificity for EGFR and ErbB2), affected the mobility of the embryos. Validation experiments with *erbb4a*-targeting antisense oligonucleotides and an *erbb4a* mutant fish line suggested a critical role for ErbB4 in mediating the effects. Mechanistic experiments further indicated that the defect in motility was associated with structural defects in the developing truncal muscle fibers, changed muscle-specific gene expression, and reduced motoneuron length.

RESULTS

Pan-ErbB kinase inhibitors suppress motility of zebrafish embryos

To address the effects of ErbB inhibition on developing tissues, 8–h past fertilization (hpf) zebrafish embryos were treated for 48 h with 10 μM of nine different ErbB TKIs. While there were no statistically significant differences in the survival of the embryos, some of the TKIs were observed to inhibit their movement. To quantitatively analyze the role of ErbB TKIs in regulating motility, touch–response assays were carried out (Granato *et al.*, 1996), and the movement of the embryos was videorecorded (an example of the procedure is shown in Supplemental Movie S1). The swim tracks for individual embryos are visualized in Figure 1A and Supplemental Figure S1. Inhibitors, such as erlotinib and gefitinib, expected to inhibit EGFR alone, did not affect either the length of the swim bursts (Figure 1B) or the average speed during the bursts (Figure 1C). A moderate and not statistically significant effect was observed with the dual-specific EGFR/ErbB2 inhibitor lapatinib (Figure 1, B and C). However, the irreversible pan-ErbB inhibitors afatinib, neratinib, canertinib, and dacomitinib, capable of suppressing the activity of EGFR, ErbB2, and ErbB4, indicated some reduction in motility, and a statistically significant effect was observed for canertinib (Figure 1). While our analysis was not sufficiently powered to detect relatively small effects, these findings suggested that inhibition of the ErbB4 kinase was associated with the reduced motility of the embryos. Indeed, the TKI AG 1478 shown to block the activity of EGFR as well ErbB4 (Levitzki and Gazit, 1995; Egeblad *et al.*, 2001) blocked motility in a statistically significant manner (Figure 1).

erbb4a is the predominant *erbb4* gene expressed during zebrafish organogenesis

To address the relative expression of the two *erbb4* genes in zebrafish, whole embryos were lysed and subjected to real-time reverse transcription-PCR (RT-PCR) analysis at different time points after fertilization. While both loci were expressed during early development, there was a switch of the predominant transcript at 24 hpf (Supplemental Figure S2A). Expression of *erbb4b* peaked at 6 hpf, the earliest time point analyzed, and declined thereafter. In contrast, *erbb4a* was expressed at a low level at 6 hpf, reached a similar level to *erbb4b* at 24 hpf, and further increased to clearly dominate over *erbb4b* at 48 hpf (Supplemental Figure S2A). Western blot analysis with anti-ErbB4 E200 against the intracellular domain of ErbB4 confirmed the expression of ErbB4 protein, and demonstrated significantly increased protein expression from 48 hpf onward (Supplemental Figure S2B). Whole mount immunofluorescence analysis with the ErbB4 antibody HFR-1 demonstrated the strongest ErbB4 expression in the brain and somites of 48-hpf embryos (Supplemental Figure S2, C–F).

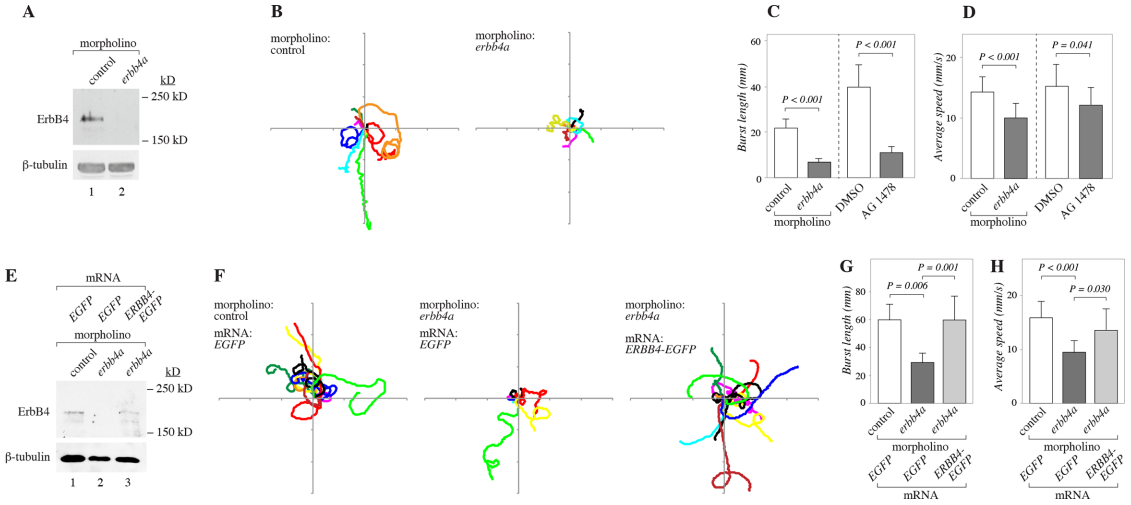

FIGURE 2: *erbb4a* is necessary for normal motility of zebrafish embryos. (A) Western blot analysis of ErbB4 expression (anti-ErbB4 E200) in 48-hpf embryos injected at the one- to eight-cell stage with *erbb4a*-targeting or control morpholino (lanes 1 and 2). β-tubulin (antibody E7) expression was analyzed from the same lysates to control loading. (B) Touch–response assays measuring motility of 48-hpf morphants and embryos treated with AG 1478 or untreated. The colored lines demonstrate videorecorded tracks of swim bursts of 10 randomly selected embryos stimulated to move by a physical touch to the tail. (C, D) Quantification of the length of the swim burst (C) and the average speed during the burst (D) in the touch–response assays. Control morpholino, $n = 32$; *erbb4a* morpholino, $n = 17$; DMSO, $n = 17$; AG 1478, $n = 18$. (E) Western blot analysis of ErbB4 expression (anti-ErbB4 E200) in 48-hpf embryos coinjected at the one- to eight-cell stage with *erbb4a* targeting or control morpholino together with in vitro transcribed mRNA encoding EGFP or a fusion protein of ErbB4 and EGFP (*ERBB4-EGFP*). β-tubulin (clone E7) expression was analyzed from the same lysates to control loading. (F) Ten randomly selected swim tracks of 48-hpf morphants subjected to touch–response assays. (G, H) Quantification of the length of the swim burst (G) and the average speed during the burst (H) in the touch–response assays. Control morpholino + *EGFP*, $n = 27$; *erbb4a* morpholino + *EGFP*, $n = 18$; *erbb4a* morpholino + *ERBB4-EGFP*, $n = 12$.

erbb4a is necessary for motility of zebrafish embryos

As an independent approach to addressing the function of *erbb4a*, morpholino antisense oligonucleotides were injected into one- to eight-cell stage embryos. A morpholino-targeting *erbb4a* mRNA reduced the amount of total ErbB4 protein present in lysate of whole embryos by 99% (Figure 2A, lanes 1 and 2), further supporting the significance of *erbb4a* as the major *ERBB4* ortholog and also validating the functionality of anti-ErbB4 E200 antibody in zebrafish.

Validation experiments with AG 1478 confirmed the observations of the ErbB kinase inhibitor screen. Similarly to treatment with AG 1478, the 48-hpf *erbb4a* morphant embryos moved for shorter distances in response to a contact, as compared with respective controls. Figure 2B demonstrates the swim bursts of 10 randomly selected embryos treated or not with either *erbb4*-targeting morpholino. Both the burst length (Figure 2C) and the average velocity during the movement (Figure 2D) were reduced in embryos with reduced ErbB4 signaling. Both ErbB4 protein expression (Figure 2E) and the effects on embryonic motility (Figure 2, F–H) were rescued by coinjecting the embryos with human *ERBB4* mRNA simultaneously with the *erbb4a*-targeting morpholino oligonucleotide, supporting the specificity of the antisense morpholino approach.

Inhibition of *erbb4a* induces structural defects in developing muscle fibers

To address a potential general effect of *erbb4a* down-regulation on development, the head–trunk angle (HTA) was analyzed as a gross measure of developmental stage (Kimmel *et al.*, 1995). No significant difference ($p = 0.99$) in HTA between embryos injected with control morpholino (average = 152 ± 13°, $n = 13$) or morpholino targeting *erbb4a* (average = 152 ± 12°, $n = 13$) was observed. However, the number of somites was significantly ($p < 0.001$) reduced in 48-hpf *erbb4a* morphants (29.6 ± 0.3 somites/embryo, $n = 18$) in comparison with the embryos treated with control morpholinos (31.2 ± 0.2 somites/embryo, $n = 17$). A similarly significant ($p < 0.001$) decrease in the number of somites was observed in AG 1478–treated embryos (29.0 ± 0.3 somites/embryo, $n = 8$) in comparison with embryos treated with the dimethyl sulfoxide (DMSO) buffer alone (30.8 ± 0.3 somites/embryo, $n = 9$).

To address the role of *erbb4a* at the level of skeletal muscle fibers, whole-mount 48-hpf embryos were stained with an anti-myosin antibody and imaged by confocal microscopy (Figure 3A). Both the AG 1478 treatment and the *erbb4a*-targeting morpholino resulted in a significantly reduced diameter of muscle fibers (Figure 3, A and B), suggesting a role for ErbB4a signaling in maintaining normal myocyte morphology.

erbb4a knockdown is associated with reduced motoneuron length but not with reduced AchR expression in the skeletal muscle

Defects in developing muscle could be secondary to impaired innervation. Indeed, ErbB4 signaling has been suggested to regulate AchR expression and function in mouse models (Rimer *et al.*, 2004; Schmidt *et al.*, 2011). However, knockdown of *erbb4a* did not result in significant changes in AchR expression in 48-hpf zebrafish embryos when measured either by real-time RT-PCR analysis of AchR subunits α1 (*chrna1*), β1 (*chrnb1*), and δ (*chrnd*) ($p = 0.08$, 0.25, and 0.86, respectively; $n = 10$) or by AchR staining with fluorescent α-bungarotoxin ($p = 0.91$ for the area covered by fluorescence signal; $n = 6$). In contrast, confocal immunofluorescence analyses of motoneurons by anti–synaptotagmin-2 (znp-1) antibody demonstrated that the motoneuronal axons of *erbb4a* morphants were

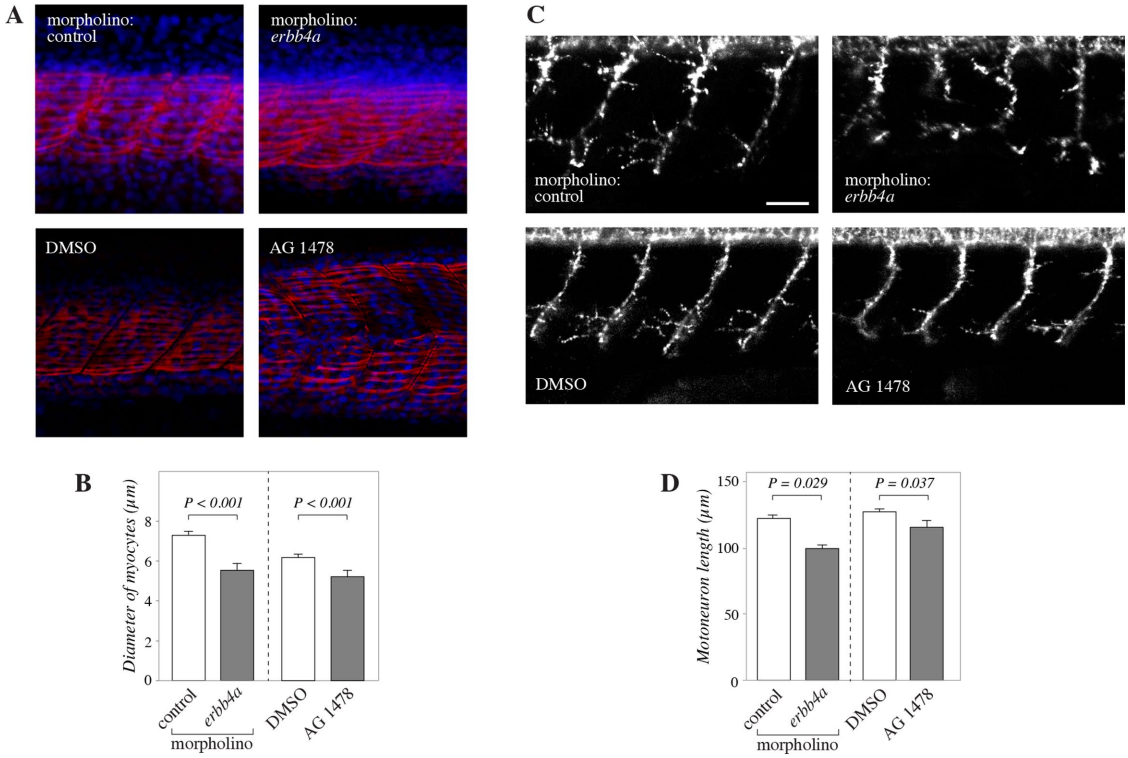

FIGURE 3: Effect of *erbb4a* knockdown on myocyte and motoneuron morphology. (A) Confocal immunofluorescence images of 48-hpf embryos treated from 8 to 48 hpf with 10 μM of the ErbB kinase inhibitor AG 1478 or the DMSO buffer alone. Whole-mount embryos were stained with the anti-myosin F59 (red) and the DNA stain 4′,6-diamidine-2-phenylindole (blue). (B) Quantification of the thickness of individual F59-positive myocytes from confocal immunofluorescence images. The number of embryos analyzed was as follows: control morpholino, $n = 14$; *erbb4a* morpholino, $n = 15$; DMSO, $n = 16$; AG 1478, $n = 15$. Ten myocytes was analyzed from each embryo. (C) Confocal immunofluorescence images of 48-hpf embryos injected at the one- to eight-cell stage with *erbb4a*-targeting or control morpholino (top panels) or treated from 8 to 48 hpf with 10 μM of the ErbB kinase inhibitor AG 1478 or the DMSO buffer alone (bottom panels). Whole-mount embryos were stained with anti–synaptotagmin-2 (znp-1) to visualize motoneurons. Scale bar, 40 μm. (D) Quantification of the length of znp-1-immunoreactive motoneuron axons from confocal immunofluorescence images. The numbers of neurons (embryos) analyzed were as follows: control morpholino, $n = 39$ (11); *erbb4a* morpholino, $n = 38$ (10); DMSO, $n = 33$ (11); AG 1478, $n = 38$ (11).

shorter than in control morpholino-injected embryos (Figure 3, C and D). Similar findings were observed with ErbB kinase inhibitor AG 1478–treated embryos (Figure 3, C and D).

Inhibition of ErbB4a alters expression of several muscle-cell specific genes

To characterize *erbb4a*-dependent signaling in the muscle fibers at the molecular level, expression of the muscle-specific myosin genes *cmcl2*, *myhc4*, *smyhc1*, and *tpm1* was analyzed from total lysates of 48-hpf embryos by real-time RT-PCR. Significantly reduced expression of *smyhc1* and *tpm1* was observed after *erbb4a* morpholino injection (Figure 4A) and AG 1478 treatment (Figure 4B). The *erbb4a*-targeting morpholino also significantly reduced the expression of *cmcl2* (Figure 4A).

Western blot analyses indicated that the steady-state expression levels of myosin proteins recognized by antibodies raised against chicken tropomyosin or chicken fast-type myosin light chain were clearly reduced in response to either *erbb4a*-targeting morpholino or AG 1478 (Figure 4C). In contrast, the myosin species recognized by antibodies raised against chicken slow-type myosin heavy chain remained unchanged after both genetic and chemical down-regulation of ErbB4 function (Figure 4C).

To elucidate the temporal requirement of ErbB activity, AG 1478 was added to the embryos at 8, 24, or 48 hpf and washed away at 24, 48, or 72 hpf. The effect on muscular tissue was assessed by Western blot analysis of tropomyosin expression at the 72-hpf time point for all treatment periods. A robust decrease in tropomyosin level was already detected when AG 1478 was administered at 8 hpf regardless of the washout time point at 24, 48, or 72 hpf (Figure 4D, lanes 2–4 vs. lane 1). An attenuated, but still clear, response was also observed at the later treatment period from 24 or 48 hpf to 72 hpf (Figure 4D, lane 5 or 6 vs. lane 1).

Rescue of reduced motility of *erbb4a* morphants by muscle-specific ERBB4 expression

To more directly address whether the reduced motility of *erbb4a*-deficient embryos was caused by a defect of developing myocytes, a construct to overexpress human *ERBB4* under the muscle-specific *acta1* promoter (Jacoby *et al.*, 2009) was cloned, as described in *Materials and Methods*. This construct, encoding both ErbB4 and EGFP, or a control construct encoding EGFP alone, was coinjected into the embryos with the *erbb4a*-targeting or control morpholino. Interestingly, the mosaic muscle cell–specific expression of ErbB4 in the 48-hpf G0 embryos was sufficient to at least partially rescue the reduction in the tropomyosin expression (Figure 5A) and the reduction of muscle fiber diameter (Figure 5, B and D), as well as the shortening of motoneuron axons (Figure 5, C and E). Moreover, the expression of the ErbB4 construct with the muscle-specific promoter

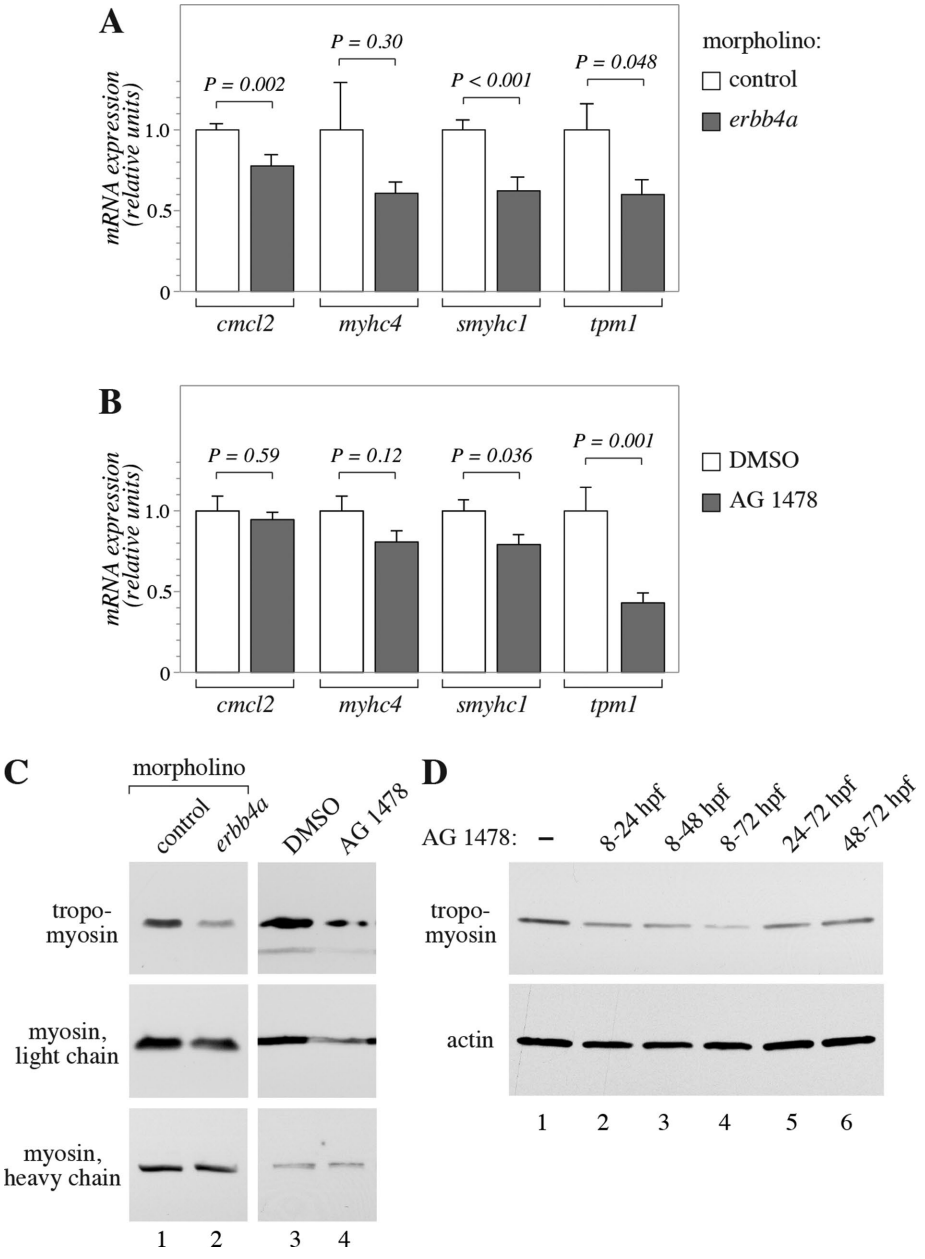

FIGURE 4: *erbb4a* is necessary for expression of several muscle-specific genes. (A, B) Real-time RT-PCR analysis of the expression of muscle-specific genes in 48-hpf embryos injected at the one- to eight-cell stage with *erbb4a*-targeting or control morpholino (A) or treated from 8 to 48 hpf with 10 µM of the ErbB kinase inhibitor AG 1478 or the DMSO buffer alone (B). Control morpholino, $n = 10$; *erbb4a* morpholino, $n = 10$; DMSO, $n = 11$; AG 1478, $n = 12$. (C) Western blot analyses of the expression of the muscle-specific proteins tropomyosin (clone CH-1), myosin light chain (clone F310), and myosin heavy chain (clone F59) in the 48-hpf embryos. (D) Western blot analysis of the expression of tropomyosin in embryos treated with 10 µM of AG 1478 for the indicated periods of time postfertilization. All other time intervals included incubation with DMSO. β-actin (sc-1616) expression was analyzed from the same lysates to control loading.

was sufficient to partially rescue the compromised motility of the *erbb4a* morphants in the touch–response assays (Figure 5, F–H).

Spontaneous motility is reduced in *erbb4a* mutant embryos

To control for the reported lack of specificity of the morpholino approach (Kok *et al.*, 2014; Rossi *et al.*, 2015), as well as potential promiscuity of chemical inhibition, an *erbb4a* mutant fish line was generated using CRISPR/*Cas*9-mediated targeted mutagenesis. We successfully isolated a 22 base pair–deletion allele of *erbb4a* (*erbb4a*^{ubs35}) (Figure 6A) that causes a frame shift and premature stop codon in the DNA sequence encoding the extracellular domain of ErbB4a. Based on in silico translation, this results in a truncated ErbB4a protein lacking transmembrane, kinase, and intracellular domains (Figure 6B). Indeed, Western blot analysis of a pool of 96-hpf mutants using the anti-ErbB4 E200 recognizing the intracellular domain of ErbB4 demonstrated protein expression levels reduced to 65% for the heterozygous *erbb4a*$^{+/ubs35}$ embryos and to 19% for the homozygous *erbb4a*$^{ubs35/ubs35}$ embryos (Figure 6C). The remaining 19% were comparable to the relative amount of the *erbb4b* transcript in the homozygous *erbb4a*$^{ubs35/ubs35}$ embryos (16% when compared with the total number of *erbb4a* + *erbb4b* transcripts in the wild-type embryos by real-time RT-PCR), suggesting that the remaining ErbB4-immunoreactive band in the mutants derived, not from ErbB4a, but from ErbB4b protein.

To measure the effect of the *erbb4a*^{ubs35} mutation on motility, an assay recording spontaneous motility for a period of 10 min was carried out (Supplemental Movie 2). Indeed, the embryos homozygous for the *erbb4a*^{ubs35} mutation (*erbb4a*$^{ubs35/ubs35}$) moved for a reduced distance, as well as at lower speed, in comparison with heterozygous *erbb4a*$^{+/ubs35}$ embryos (Figure 6, D–F).

DISCUSSION

Treatment with pan-ErbB TKIs was observed to reduce the motility of developing zebrafish embryos. Several lines of evidence indicate that these effects were mediated, at least partially, by ErbB4. Chemical inhibition of the ErbB kinase activity, as well as genetic targeting of *erbb4a*, resulted in decreased motility of embryos, reduction of the diameter of muscle fibers, and reduced expression of the myosin genes *cmcl2*, *smyhc1*, and *tpm1*. The defects in the motility of the embryos were partially rescued by muscle-specific mosaic expression of human *ERBB4*, implying a requirement for ErbB4 expressed by the myofibers for the development of skeletal muscle. Consistently, the motility of embryos with targeted *erbb4a* was reduced both in touch–response assays and in assays measuring spontaneous swimming.

Therapeutic TKIs may promote off-target effects by inhibition of other structurally homologous kinases. Here, we observed similar defects in motility using different ErbB kinase inhibitors, as well as by antisense oligonucleotide and mutational approaches targeting *erbb4a*, indicating that the effects on motility were indeed on-target and specific for blocking ErbB4 signaling.

To confirm the expression of *erbb4a* (and *erbb4b*) in zebrafish independent of the use of antibodies, we analyzed relevant RNA-seq

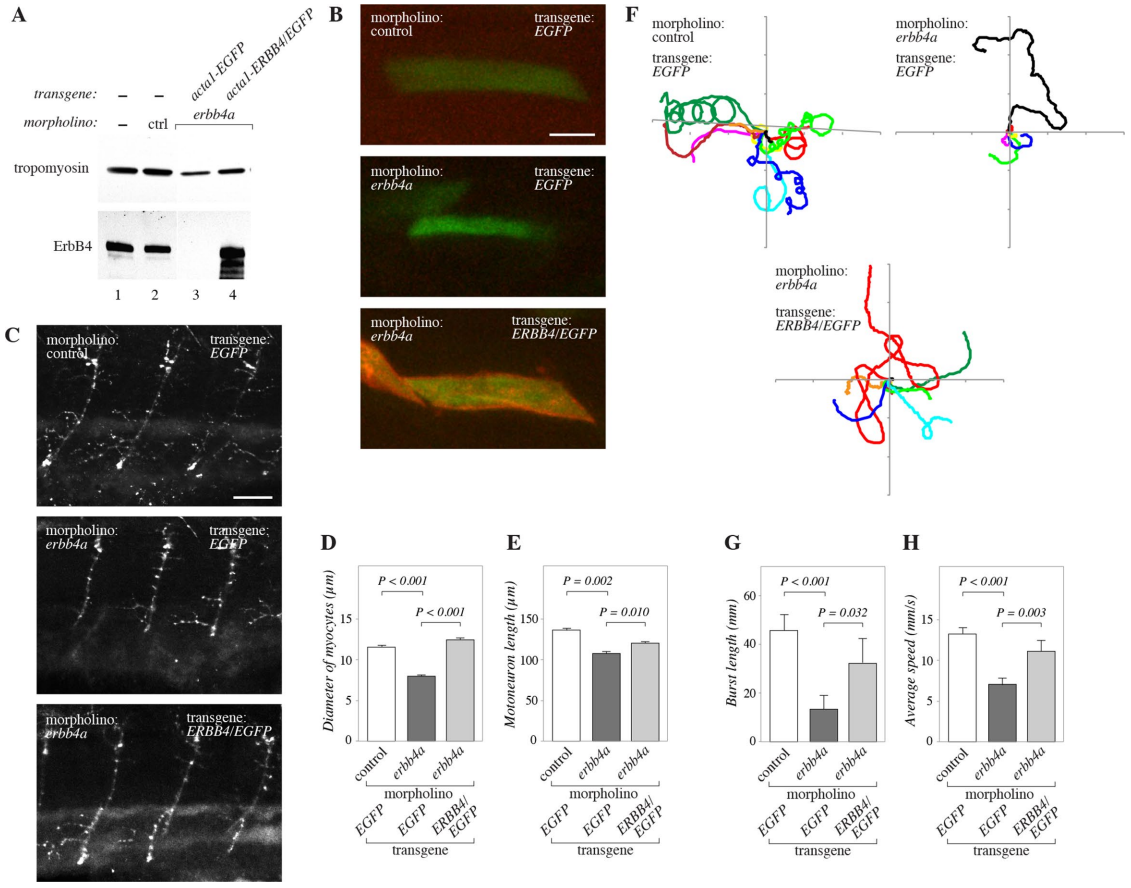

FIGURE 5: Muscle-specific expression of *ERBB4* can rescue neuromuscular phenotypes in *erbb4a* morphants. Analyses of 48-hpf embryos coinjected at the one- to eight-cell stage with *erbb4a*-targeting or control morpholino together with constructs encoding EGFP, or ErbB4 and EGFP (*ERBB4/EGFP*), under the muscle-specific *acta1* promoter. (A) Western blot analysis of ErbB4 expression (anti-ErbB4 E200). Tropomyosin (clone CH1) expression was analyzed from the same lysates. All the samples were run on the same gels, but some nonrelevant lanes were omitted between samples 2 and 3, as indicated by white line. (B) Confocal whole-mount immunofluorescence analysis of GFP-positive mosaic muscle cells. GFP = green; anti-ErbB4 (E200) = red. Scale bar, 20 μm. (C) Confocal whole-mount immunofluorescence analysis of motoneurons with anti–synaptotagmin-2 (znp-1) antibody. Scale bar, 40 μm. (D) Quantification of the thickness of individual GFP-positive myocytes from confocal immunofluorescence images (representative images shown in B). The numbers of GFP-expressing myocytes (embryos) analyzed were as follows: control morpholino + *EGFP*, $n = 28$ (5); *erbb4a* morpholino + *EGFP*, $n = 65$ (5); *erbb4a* morpholino + *ERBB4/EGFP*, $n = 26$ (5). (E) Quantification of the length of motoneuron axons from confocal immunofluorescence images (representative images shown in C). The numbers of neurons (embryos) analyzed were as follows: control morpholino + *EGFP*, $n = 24$ (8); *erbb4a* morpholino + *EGFP*, $n = 29$ (9); *erbb4a* morpholino + *ERBB4/EGFP*, $n = 18$ (6). (F) Ten randomly selected swim tracks of touch–response assays with 48-hpf morphants expressing the rescue constructs encoding EGFP, or ErbB4 and EGFP (*ERBB4/EGFP*), under the muscle-specific acta1 promoter. (G, H) Quantification of the length of the swim burst (G) and the average speed during the burst (H) in the touch–response assays. Control morpholino + *EGFP*, $n = 32$; *erbb4a* morpholino + *EGFP*, $n = 15$; *erbb4a* morpholino + *ERBB4/EGFP*, $n = 20$.

data sets available in repositories. In the embryonic brain (whole dissected head), the *erbb4a* expression was relatively high (*erbb4a*: 2.86 [range 2.59–3.13] FPKM; *erbb4b*: 1.53 [1.28–1.78] FPKM; Borck *et al.*, 2015). In adult muscle, *erbb4a* was also clearly expressed (*erbb4a*: 0.72 [0.58–0.87] FPKM; *erbb4b*: 0.76 [0.56–0.97] FPKM; Louie *et al.*, 2017). In FACS-purified spinal cord neurons, *erbb4a* mRNA was expressed at very low level, if at all (*erbb4a*: 0.016 [0–0.07] FPKM; *erbb4b*: 0.11 [0–0.23] FPKM; Friedmann *et al.*, 2015). Taken together, the expression pattern from our immunofluorescence analysis was in line with published RNA-seq expression data.

ErbB4 has previously been demonstrated to be expressed in human (Plowman *et al.*, 1993; Junttila *et al.*, 2005), mouse (Elenius *et al.*, 1997), and rat (Lebrasseur *et al.*, 2003) skeletal muscle tissue. In the rodent myocytes, ErbB4 protein is concentrated in the neuromuscular junctions, where it has been suggested to act as a postsynaptic neuregulin receptor (Zhu *et al.*, 1995; Trinidad *et al.*, 2000). The neuromuscular junctions are superficially normal and functional in mice lacking both *Erbb2* and *Erbb4* in the skeletal muscle (Escher *et al.*, 2005). However, detailed analysis has demonstrated altered AchR recycling and signal transmission in the neuromuscular junctions in the muscles of mice lacking both *Erbb2* and *Erbb4* (Schmidt *et al.*, 2011). ErbB4 has also been shown to activate AchR transcription in cultured rodent myotubes (Rimer *et al.*, 2004). Although our real-time RT-PCR and bungarotoxin labeling analyses failed to demonstrate significant quantitative changes in AchR expression, it remains to be elucidated whether AchR recycling or signaling is affected in the *erbb4a*-deficient zebrafish model.

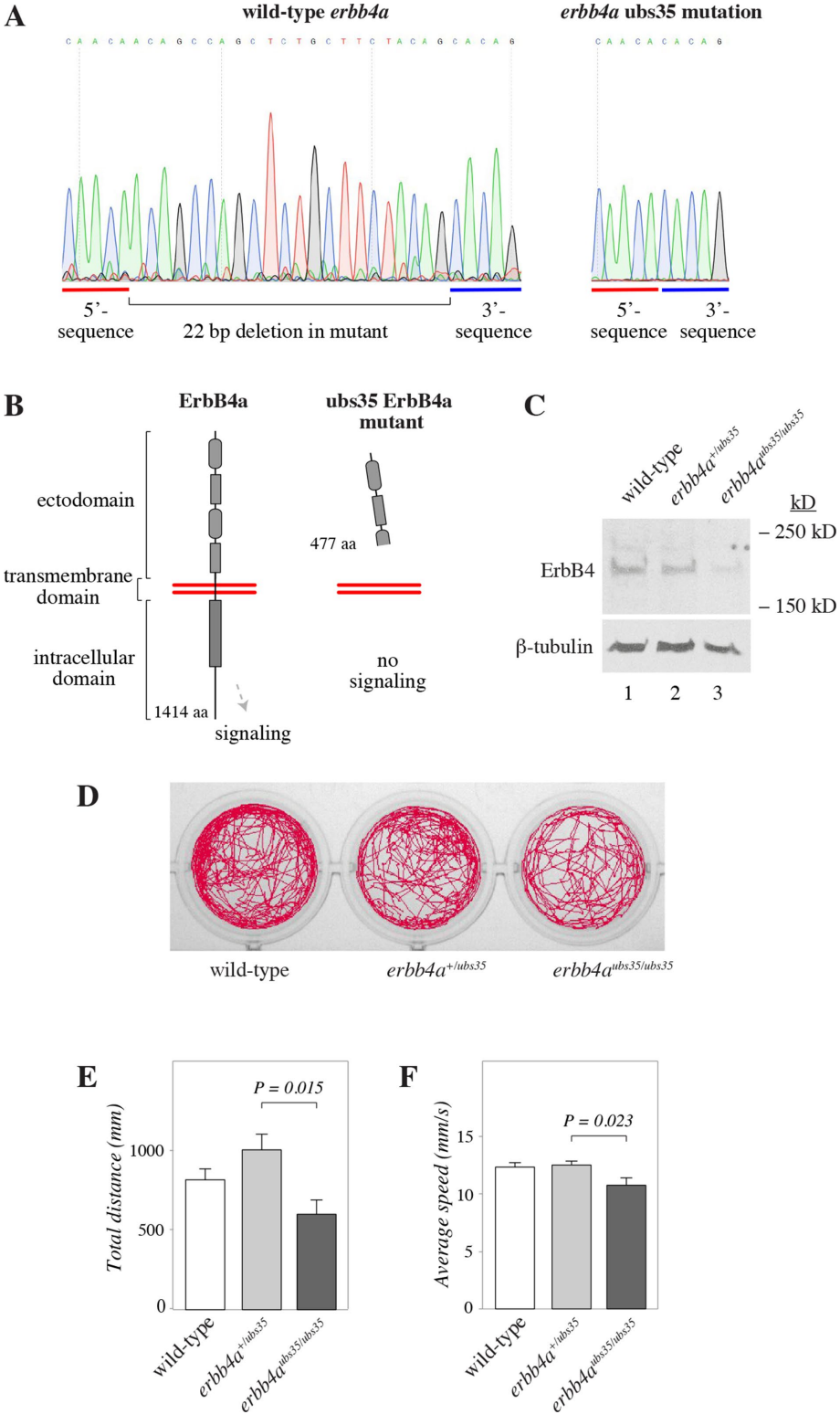

FIGURE 6: Defective motility in *erbb4a* mutant embryos. (A) Sanger sequencing data of wild-type and mutant *erbb4a*^{ubs35} alleles. Red and blue lines indicate 5′ and 3′ sequences flanking the mutation site, respectively. The black bracket in the wild-type sequence indicates the deletion site and sequence missing from the ubs35 mutant allele of *erbb4a*. (B) Schematic presentation of wild-type and mutant ErbB4a proteins. (C) Western blot analysis of ErbB4 expression in 96-hpf wild-type and heterozygote (*erbb4a*$^{+/ubs35}$) and homozygote (*erbb4a*$^{ubs35/ubs35}$) mutant embryos. Five to six embryos per genotype were pooled for Western analysis. (D–F) Spontaneous motility assay. Ninety-six-hpf zebrafish embryos were analyzed for spontaneous motility in 24-well plates (1 embryo/well) using a DanioVision instrument. (D) Tracks of swimming over a period of 10 min. (E, F) Quantification of the length of the swim tracks (E) and the average speed (F). Wild-type *erbb4a*, $n = 13$; heterozygote *erbb4a*$^{ubs35/+}$, $n = 18$; homozygote *erbb4a*$^{ubs35/ubs35}$, $n = 13$.

ErbB-targeting TKIs are being tested in several early clinical trials for pediatric malignancies, such as leukemias, brain malignancies, and osteosarcomas (www.clinicaltrials.gov). While the extent to which ErbB TKIs provoke adverse neuromuscular effects in pediatric patients remains to be addressed, muscle spasms and musculoskeletal pain are among the common side effects associated with the ErbB4-targeting pan-ErbB inhibitors, such as afatinib, neratinib, and dacomitinib, in adult patients (Yang *et al.*, 2012; Chan *et al.*, 2016; Wu *et al.*, 2017). Interestingly, inhibitory mutations in the *ERBB4* gene have been linked to familial and sporadic amyotrophic lateral sclerosis (ALS; Takahashi *et al.*, 2013), a disease characterized by both motoneuron loss and muscle atrophy (Al-Chalabi *et al.*, 2012). These findings suggest a role of ErbB signaling, and specifically ErbB4, in the regulation of neuromuscular function also in humans.

Taken together, our observations indicate that ErbB4 inhibition promotes neuromuscular toxicity in developing zebrafish. These findings underline the need to characterize the toxicological properties of novel molecularly targeted therapeutics used for pediatric patients.

MATERIALS AND METHODS

Fish culture

Wild-type zebrafish (*D. rerio*) were maintained according to standard procedures (Nüsslein-Volhard and Dahm, 2002) in the aquatic facilities of the Laboratory of Animal Physiology, University of Turku; Laboratory of Aquatic Pathobiology, Åbo Akademi University; and Biozentrum, University of Basel. The embryos were cultured at 28.5°C in E3 medium (5 mM NaCl, 0.17 mM KCl, 0.33 mM $CaCl_2$, 0.33 mM $MgSO_4$, 0.01% methylene blue). In samples analyzed by fluorescence microscopy, pigmentation was inhibited by the addition of 0.2 mM phenylthiourea (Sigma) into the E3 medium. Housing of adult zebrafish and experiments with zebrafish embryos were performed according to the European Convention for the Protection of Vertebrate Animals Used for Experimental and Other Scientific Purposes, Statutes 1076/85 and 62/2006 of The Animal Protection Law in Finland, EU Directive 86/609, and Swiss national guidelines of

animal experimentation (TSchV) under licenses MMM/465/712-93 (issued by the Ministry of Agriculture and Forestry, Finland) and 1014H and 1014G1 (issued by the Veterinäramt-Basel-Stadt).

ErbB tyrosine kinase inhibitors

To block ErbB kinase activity in the embryos, 10 μM of tyrosine kinase inhibitors AG 1478 (Calbiochem), erlotinib, gefitinib, lapatinib, afatinib, neratinib, canertinib (all from Santa-Cruz Biotechnologies), osimertinib, and dacomitinib (both from Cayman Chemical), diluted in DMSO, or DMSO alone was applied in E3 medium at 8 hpf, except as indicated for experimentation shown in Figure 4D. The final concentration of DMSO was 0.1% of the culture medium.

Morpholino antisense oligonucleotides

To block endogenous expression of *erbb4a* in zebrafish embryos, a morpholino antisense oligonucleotide targeting the translation initiation site of the *erbb4a* mRNA (5′-AGAAGGAAGCGAACCGGCCACATTT-3′) and a standard control morpholino targeting a mutated splice site of human β-globin mRNA (5′-CCTCTTACCTC AGTTACAATTTATA-3′) were purchased from Gene Tools LLC. The 25 nucleotide–long antisense morpholino sequence contained 15 mismatches with *erbb4b* and 12 mismatches with human *ERBB4*.

DNA constructs and mRNA production

To generate the fusion expression plasmid *pcDNA3.1ERBB4EGFP*, a *Bgl*II/*Not*I fragment of *pERBB4-EGFP* (Williams *et al.*, 2004) including an insert encoding human ErbB4 (nucleotides 99-3974; NM_001042599.1) fused to EGFP was blunted and ligated into the *Eco*RV site of *pcDNA3.1*. A *Not*I/*Xba*I fragment of pCS2FA-transposase (Kwan *et al.*, 2007) encoding the Tol2 transposon was inserted into *pcDNA3.1* (Invitrogen) to generate *pcDNA3.1Tol2*. RNA was transcribed in vitro from template plasmids *pcDNA3.1EGFP* (kind gift from Chris Cartwright, Stanford University, Stanford, CA), *pcDNA3.1ERBB4EGFP* (human *ERBB4*), or *pcDNA3.1Tol2* using T7 RNA polymerase and mScript mRNA production system (Epicentre). Poly A tails and 5′ cap structures were synthesized using mScript mRNA production system (Epicentre).

Plasmids for zebrafish transgenesis were cloned using the Tol2kit system (Kwan *et al.*, 2007). The expression constructs *pDestTol2A2-acta1-EGFPpA* for expression of the *EGFP* under the muscle-specific *acta1*-promoter was generated in a Gateway LR recombination reaction including *pDestTol2A2* (Kwan *et al.*, 2007), *p5E-acta1* (Jacoby *et al.*, 2009), *pME-EGFP* (Kwan *et al.*, 2007), and *p3E-EGFPpA*, using previously described methods (Kwan *et al.*, 2007). The plasmid *p3EP2AEGFPpA* encoding the self-cleaving peptide P2A from porcine teschovirus fused to *EGFP* was generated from *p3E-EGFPpA* (Kwan *et al.*, 2007) by PCR using the primers 5′-CAGGCTGGAGACGTGGAGGAGAACCCTGGACCTGTGAGCAAGGGCGAG-GAGCTGTTCAC-3′ and 5′-CTTCAGCAGGCTGAAGTTAGTA GCTCCGCTTCCCA-TGGTGGCCACTTTGTACAAGAAAG-3′. The P2A peptide allows the expression of two proteins under the same promoter, and is functional in zebrafish (Kim *et al.*, 2011). The expression constructs *pDestTol2A2-acta1-ERBB4-P2A-EGFPpA* for expression of human ErbB4 together with EGFP under the muscle-specific acta1-promoter was generated in a recombination reaction including *pDestTol2A2*, *p5E-acta1*, *pDONR223-ERBB4* (Addgene plasmid 23875; Johannessen *et al.*, 2010), and *p3EP2AEGFPpA*.

Microinjection of morpholino oligonucleotides, mRNAs, and DNA constructs

Embryos at the one- to eight-cell stage were microinjected using Femtotip glass capillary needles (Eppendorf) and a Femtojet pressure system (Eppendorf) equipped with an Injectman2 micromanipulator (Eppendorf) attached to a StereoLumarV.12 stereomicroscope (Zeiss). Injection volume was calculated by injecting a small droplet into halocarbon oil. The diameter of the droplet was measured and the volume calculated.

Volumes of 2–4 nl were used in injections. Morpholinos and in vitro transcribed mRNAs were injected into the yolk at final concentrations of 7.5 ng/embryo (lowest dose to cause robust *erbb4a* knockdown at 48 hpf) and 500 pg/embryo, respectively. DNA constructs were injected into the yolk at a final concentration of 125 pg/embryo together with 120 pg/embryo of in vitro transcribed *Tol2* transposon mRNA.

CRISPR/Cas9-mediated targeting of endogenous *erbb4a* locus

The guide RNA specific for the *erbb4a* locus was designed using ChopChop online software (Montague *et al.*, 2014; Labun *et al.*, 2016; (http://chopchop.cbu.uib.no/). The preparation of single-guide RNA (sgRNA) and its injection into one- to four-cell stage embryos were performed as previously described (Gagnon *et al.*, 2014). In brief, an *erbb4a*-targeting DNA oligonucleotiude (5′-TTCTAATACGACTCACTATAGAAGCAGAGCTGGCTGTTGTGTTTTAGAGCTAGA-3′) was annealed with the DNA oligonucleotide (5′-AAAAGCA CCGACTCGGTGCCACTTTTTCAAGTTGATAACGGACTAGCCTTATTTTAACTTGCTATTTCTAGCTCTAAAAC-3′). The annealed oligonucleotides were filled in using Phusion DNA polymerase. The gel-purified DNA fragment was then used as a substrate for the in vitro RNA transcription reaction with T7 RNA polymerase (MAXIscript T7 Transcription Kit; Ambion). The resulting sgRNA was precipitated with ethanol and ammonium acetate and dissolved in RNase-free water. Purified sgRNA was complexed with recombinant Cas9 protein (Gagnon *et al.*, 2014) and injected into one- to four-cell stage embryos of the Tu zebrafish strain. The injected embryos were grown into adulthood and outcrossed with wild-type fish. The founder fish (G0) were identified by screening the offspring for the presence of mutations in *erbb4a* locus using PCR amplification and digestion with T7 endonuclease or *Alu*I (both from New England Biolabs). A 22 base pair–deletion allele (*erbb4a*^{ubs35}) was successfully isolated and F3 generation was used in the experiments. The *erbb4a* genotyping PCR was carried out as nested PCR with outer primer pair (5′-ACTCTGGTTCATTGAAACGTCA-3′; 5′-CAT CATGCATCAGAGTGCCAAG-3′) and inner primer pair (5′-ATCAACACATGCTGTATCTGCTCT-3′; 5′-CTTGATAGGAA AGTGCAGCGAG-3′) using Taq DNA polymerase (New England Biolabs). To obtain DNA, RNA, and protein samples from the same individual embryos to allow first genotyping and then pooling samples, a NucleoSpin TriPrep kit (Macherey-Nagel) was used.

Protein extraction and Western blotting

Five to twenty embryos were homogenized using a handheld motorized pellet pestle (Sigma) in lysis buffer (1% Triton X-100, 10 mM Tris-HCl, pH 7.4, 1 mM EDTA, 2 mM phenyl methyl sulfonyl fluoride, 10 μg/ml aprotinin, and 10 μg/ml leupeptin) or directly in sample buffer (2% SDS, 10% glycerol, 60 mM Tris-HCl, pH 6.8, 100 mM dithiothreitol, and 0.01% bromophenol blue). Homogenates were centrifuged for 15 min at 12,000 × *g* at 4°C. Supernatants were analyzed by Western blotting, as previously described (Kainulainen *et al.*, 2000), using the following primary and secondary antibodies: anti-ErbB4 (E200; Abcam), anti–β-tubulin (clone E7), anti–slow muscle myosin heavy chain (clone F59), anti–fast muscle myosin light chain (clone F310), anti-tropomyosin (clone CH1), anti–β-actin (sc-1616; Santa Cruz Biotechnology), horseradish peroxidase (HRP)-conjugated goat anti-rabbit (sc-2004; Santa Cruz Biotechnology),

HRP-conjugated goat anti-mouse (sc-2005; Santa Cruz Biotechnology), and HRP-conjugated rabbit anti-goat (sc-2768; Santa Cruz Biotechnology). Anti–β-tubulin, anti-myosin, anti-tropomyosin, and anti–synaptotagmin-2 (znp-1) monoclonal antibodies developed by M. Klymkowsky, F. E. Stockdale, J.J.-C. Lin, and B. Trevarrow, respectively, were obtained from the Developmental Studies Hybridoma Bank developed under the auspices of the National Institute of Child Health and Human Development and maintained by the Department of Biology, University of Iowa, Iowa City.

RNA extraction and real-time RT-PCR

RNA was extracted from one to four embryos homogenized into Trisure RNA extraction reagent (Bioline Reagents) supplemented with 10 µg/ml glycogen (Roche), as recommended by the manufacturer. cDNA was synthesized using the RevertAid H-Reverse Transcription kit (Fermentas). Real-time RT-PCR analyses of diluted (1:5) cDNA samples were carried out using ABI 7900HT (Applied Biosystems) and the following primers and probes: *erbb4a*, 5′-AAACCGCAACTTGTCTTTCC-3′, 5′-CCAGAGGAAGATAGTCAAACTGG-3′, probe #21; *erbb4b*, 5′-ATGTGCATCCCCTGCACT-3′, 5′-CGTCTGAAGGCTGGCAGT-3′, probe #43; *rpl13a*, 5′-GCGGACCGATTCAATAAGGG-3′, 5′-GAAAGACGACCGAGGTGAGA-3′, probe #147; *cmcl2*, 5′-CAGGAGCCCAGACCAACA-3′, 5′-AGCAGTTTTCCCCCTCTTG-3′, probe #112; *myhc4*, 5′-CAAGCA GAAGCAGCGTGA-3′, 5′-GGGTAGCACAAAGCCTTCAG-3′, probe #82; *smyhc1*, 5′-TGCCAAGACCATCAGAAATG-3′, 5′-CACACCAAAGTGAATTCGGATA-3′, probe #52; *tpm1*, 5′-GAACGCCTTGGACAGAGC-3′, 5′-TTCCAACTGAATTAGTTCGTCTTCT-3′, probe #30; *chrna1*, 5′-TGTGTTTTACCTGCCCACAG-3′, 5′-GATCAACTCGACGATCACCA-3′, probe #15; *chrnb1*, 5′-CGAGTACTTCATCCGCAAGC-3′, 5′-ACCGTCAGGCTGGTATCTGT-3′, probe #103; *chrnd*, 5′-TCATTGTGTTGAACCTGCATT-3′, 5′-GGAAGACGCTCCAAAA AGAA-3′, probe #107. All primers were obtained from Oligomer (Helsinki, Finland), and probes were Universal ProbeLibrary probes from Roche Applied Sciences.

Immunofluorescence staining

Forty-eight-hpf embryos were fixed with 4% paraformaldehyde (PFA) in phosphate-buffered saline (PBS) overnight at 4°C, or with 100% methanol for 20 min at –20°C. The samples were rehydrated in successive 5-min incubations in solutions containing 100%, 75%, 50%, 25%, and 0% methanol in PBST (0.1% Tween-20 in PBS). Nonspecific binding was blocked in 5% goat serum (Life Technologies) in PBST for 3 h at 4°C. The samples were incubated overnight at 4°C with the primary antibodies anti-myosin heavy chain (F59), anti-ErbB4 (HFR-1; Abcam), or anti–synaptotagmin-2 (znp-1; Developmental Studies Hybridoma Bank) diluted in 5% goat serum. After four washes with PBST, the secondary antibodies goat anti-mouse Alexa 488 and goat anti-mouse Alexa 555 (Life Technologies) in 5% goat serum were applied to embryos for 3 h at room temperature. After four washes with PBST, the embryos were mounted in 87% glycerol for imaging with an LSM510 META confocal microscope (Zeiss) or with a StereoLumar V.12 stereomicroscope (Zeiss).

To stain for acetylcholine receptors (AchR), embryos were fixed with 4% PFA for 2 h at room temperature, permeabilized with water for 4 h at 4°C, and treated with 1 mg/ml collagenase for 45 min at room temperature. After three washes with PBS, nonspecific binding was blocked with PBDT (PBS, 1% bovine serum albumin, 1% DMSO, 0.5% Triton X-100) supplemented with 5% goat serum for 1 h. To visualize AchRs, Alexa-555 labeled α-bungarotoxin (Life Technologies) was added to blocking solution and the incubation was continued for 3 h at room temperature. After four washes with PBDT, the embryos were mounted in glycerol and imaged with a Zeiss LSM 510 confocal microscope.

Image processing and analysis were performed using FIJI software. Noise in all confocal images was reduced using a median filter (2 × 2), and the contrast and brightness of images were adjusted. Bungarotoxin-alexa-555 stainings were quantified using median 2 × 2 filtering, local thresholding (radius 7), and the particle analysis tool in FIJI (particle size > 4).

Touch–response assay and digital video motion analysis

To analyze the motility of the zebrafish embryos, a touch–response assay was used (Granato *et al.*, 1996). Dechorionated 48-hpf embryos were placed in E3 medium and allowed to accommodate to room temperature. The embryos were gently touched at the tail with a plastic inoculation loop, and the subsequent swim burst was recorded with a digital video camera. Files were converted into AVI format, and image analysis was performed using ImageJ and the ParticleTracker plug-in (written by Fabrice Cordelieres, Institute Curie, Orsay, France; http://rsb.info.nih.gov/ij/plugins/track/track.html). Both the distance of the swim burst as well as the average velocity during the burst were recorded. Embryos that did not show any response to touch were excluded from further analyses.

Assay measuring spontaneous swimming and digital video motion analysis

To analyze the motility of *erbb4a* mutant embryos in the absence of physical touch, a DanioVision (Noldus IT) instrument equipped with controlled lighting was utilized. The 96-hpf embryos were assayed in 24-well plates (1 embryo/well). The plate was subjected to 5 min of light, followed by 5 min of darkness. The movement of the embryos was recorded throughout the experiment. The embryos were automatically tracked using Ethovision XT software, and the moved distance and velocity were measured. After experimentation, the embryos were genotyped as described above.

Statistical analyses

Two sample comparisons were performed using Student's *t* test and three sample comparisons using analysis of variance (ANOVA) followed by Dunnet's *t* post hoc test (IBM SPSS Statistics 20 and GraphPad Prism version 6.05). To improve the fit of data into the normal distribution, the touch response data presented in Figure 6, G and H, were subjected to transformation by natural logarithm prior to ANOVA and Dunnet's *t* post hoc test. Columns in figures indicate average + standard error.

Bioinformatic analysis of RNA-seq data

Preexisting RNA-seq data sets were analyzed using Chipster software v3.12 (Kallio *et al.*, 2011). In brief, the FASTQ files (SRR5115715, SRR1648855, and SRR1616929) were retrieved from Sequence Read Archive (www.ncbi.nlm.nih.gov/sra), and the reads were aligned against the Ensembl genome assembly of the *D. rerio* genome (Danio_rerio.GRCz10.90) using TopHat2 (Kim *et al.*, 2013). This was followed by a reference-based assembly of transcripts using Cufflinks (Trapnell *et al.*, 2010). FPKM (fragments per kilobase of exon model per million reads mapped) values were used to report the expression levels.

ACKNOWLEDGMENTS

We thank Erica Nyman, Maria Tuominen, Minna Santanen, and Nina Vuori for excellent technical assistance and Deepankar Chakroborty with help in video editing. We acknowledge the Cell Imaging Core, the Finnish Functional Genomics Centre, and the Zebrafish Core Facility (Turku Centre for Biotechnology, University of Turku and Åbo Akademi University).

REFERENCES

Al-Chalabi A, Jones A, Troakes C, King A, Al-Sarraj S, van den Berg LH (2012). The genetics and neuropathology of amyotrophic lateral sclerosis. Acta Neuropathol 124, 339–352.

Arteaga CL, Engelman JA (2014). ERBB receptors: from oncogene discovery to basic science to mechanism-based cancer therapeutics. Cancer Cell 25, 282–303.

Borck G, Hög F, Dentici ML, Tan PL, Sowada N, Medeira A, Gueneau L, Thiele H, Kousi M, Lepri F, *et al.* (2015). BRF1 mutations alter RNA polymerase III-dependent transcription and cause neurodevelopmental anomalies. Genome Res 25, 155–166.

Chan A, Delaloge S, Holmes FA, Moy B, Iwata H, Harvey VJ, Robert NJ, Silovski T, Gokmen E, von Minckwitz G, *et al.* (2016). Neratinib after trastuzumab-based adjuvant therapy in patients with HER2-positive breast cancer (ExteNET): a multicentre, randomised, double-blind, placebo-controlled, phase 3 trial. Lancet Oncol 17, 367–377.

Egeblad M, Mortensen OH, van Kempen LC, Jäättelä M (2001). BIBX1382BS, but not AG1478 or PD153035, inhibits the ErbB kinases at different concentrations in intact cells. Biochem Biophys Res Commun 281, 25–31.

Elenius K, Corfas G, Paul S, Choi CJ, Rio C, Plowman GD, Klagsbrun M (1997). A novel juxtamembrane domain isoform of HER4/ErbB4. Isoform-specific tissue distribution and differential processing in response to phorbol ester. J Biol Chem 272, 26761–26768.

Escher P, Lacazette E, Courtet M, Blindenbacher A, Landmann L, Bezakova G, Lloyd KC, Mueller U, Brenner HR (2005). Synapses form in skeletal muscles lacking neuregulin receptors. Science 308, 1920–1923.

Friedmann D, Hoagland A, Berlin S, Isacoff EY (2015). A spinal opsin controls early neural activity and drives a behavioral light response. Curr Biol 25, 69–74.

Gagnon JA, Valen E, Thyme SB, Huang P, Akhmetova L, Pauli A, Montague TG, Zimmerman S, Richter C, Schier AF (2014). Efficient mutagenesis by Cas9 protein-mediated oligonucleotide insertion and large-scale assessment of single-guide RNAs. PLoS One 9, e98186.

Granato M, van Eeden FJ, Schach U, Trowe T, Brand M, Furutani-Seiki M, Haffter P, Hammerschmidt M, Heisenberg CP, Jiang YJ, *et al.* (1996). Genes controlling and mediating locomotion behavior of the zebrafish embryo and larva. Development 123, 399–413.

Holbro T, Hynes NE (2004). ErbB receptors: directing key signaling networks throughout life. Annu Rev Pharmacol Toxicol 44, 195–217.

Jacoby AS, Busch-Nentwich E, Bryson-Richardson RJ, Hall TE, Berger J, Berger S, Sonntag C, Sachs C, Geisler R, Stemple DL, *et al.* (2009). The zebrafish dystrophic mutant softy maintains muscle fibre viability despite basement membrane rupture and muscle detachment. Development 136, 3367–3376.

Johannessen CM, Boehm JS, Kim SY, Thomas SR, Wardwell L, Johnson LA, Emery CM, Stransky N, Cogdill AP, Barretina J, *et al.* (2010). COT drives resistance to RAF inhibition through MAP kinase pathway reactivation. Nature 468, 968–972.

Junttila TT, Sundvall M, Lundin M, Lundin J, Tanner M, Härkönen P, Joensuu H, Isola J, Elenius K (2005). Cleavable ErbB4 isoform in estrogen receptor-regulated growth of breast cancer cells. Cancer Res 65, 1384–1393.

Kainulainen V, Sundvall M, Määttä J, Santiestevan E, Klagsbrun M, Elenius K (2000). A natural ErbB4 isoform that does not activate phosphoinositide 3-kinase mediates proliferation but not survival or chemotaxis. J Biol Chem 275, 8641–8649.

Kallio MA, Tuimala JT, Hupponen T, Klemelä P, Gentile M, Scheinin I, Koski M, Käki J, Korpelainen EI (2011). Chipster: user-friendly analysis software for microarray and other high-throughput data. BMC Genomics 12, 507.

Kearns GL, Abdel-Rahman SM, Alander SW, Blowey DL, Leeder JS, Kauffman RE (2003). Developmental pharmacology—drug disposition, action, and therapy in infants and children. N Engl J Med 349, 1157–1167.

Kim D, Pertea G, Trapnell C, Pimentel H, Kelley R, Salzberg SL (2013). TopHat2: accurate alignment of transcriptomes in the presence of insertions, deletions and gene fusions. Genome Biol 14, 0–9.

Kim JH, Lee S-R, Li L-H, Park H-J, Park J-H, Lee KY, Kim M-K, Shin BA, Choi S-Y (2011). High cleavage efficiency of a 2A peptide derived from porcine teschovirus-1 in human cell lines, zebrafish and mice. PLoS One 6, e18556.

Kimmel C, Ballard W, Kimmel S, Ullmann B, Schilling T (1995). Stages of embryonic development of the zebrafish. Dev Dyn 203, 253–310.

Kok FO, Shin M, Ni CW, Gupta A, Grosse AS, van Impel A, Kirchmaier BC, Peterson-Maduro J, Kourkoulis G, Male I, *et al.* (2014). Reverse genetic screening reveals poor correlation between morpholino-induced and mutant phenotypes in zebrafish. Dev Cell 1–12.

Kwan KM, Fujimoto E, Grabher C, Mangum BD, Hardy ME, Campbell DS, Parant JM, Yost HJ, Kanki JP, Chien CB (2007). The Tol2kit: a multisite gateway-based construction Kit for Tol2 transposon transgenesis constructs. Dev Dyn 236, 3088–3099.

Labun K, Montague TG, Gagnon JA, Thyme SB, Valen E (2016). CHOP-CHOP v2: a Web tool for the next generation of CRISPR genome engineering. Nucleic Acids Res 44, W272–W276.

Lebrasseur NK, Coté GM, Miller TA, Fielding RA, Sawyer DB (2003). Regulation of neuregulin/ErbB signaling by contractile activity in skeletal muscle. Am J Physiol Cell Physiol 284, C1149–C1155.

Levitzki A, Gazit A (1995). Tyrosine kinase inhibition: an approach to drug development. Science 267, 1782–1788.

Lohi O, Parikka M, Rämet M (2013). The zebrafish as a model for paediatric diseases. Acta Paediatr Int J Paediatr 102, 104–110.

Louie KW, Saera-Vila A, Kish PE, Colacino JA, Kahana A (2017). Temporally distinct transcriptional regulation of myocyte dedifferentiation and Myofiber growth during muscle regeneration. BMC Genomics 18, 854.

MacRae CA, Peterson RT (2015). Zebrafish as tools for drug discovery. Nat Rev Drug Discov 14, 721–731.

Montague TG, Cruz JM, Gagnon JA, Church GM, Valen E (2014). CHOP-CHOP: a CRISPR/Cas9 and TALEN web tool for genome editing. Nucleic Acids Res 42, W401–W407.

Nüsslein-Volhard C, Dahm R (2002). Zebrafish: A Practical Approach, New York: Oxford University Press.

Plowman GD, Culouscou JM, Whitney GS, Green JM, Carlton GW, Foy L, Neubauer MG, Shoyab M (1993). Ligand-specific activation of HER4/p180erbB4, a fourth member of the epidermal growth factor receptor family. Proc Natl Acad Sci USA 90, 1746–1750.

Reischauer S, Levesque MP, Nüsslein-Volhard C, Sonawane M (2009). Lgl2 executes its function as a tumor suppressor by regulating ErbB signaling in the zebrafish epidermis. PLoS Genet 5, e1000720.

Rimer M, Prieto AL, Weber JL, Colasante C, Ponomareva O, Fromm L, Schwab MH, Lai C, Burden SJ (2004). Neuregulin-2 is synthesized by motor neurons and terminal Schwann cells and activates acetylcholine receptor transcription in muscle cells expressing ErbB4. Mol Cell Neurosci 26, 271–281.

Rossi A, Kontarakis Z, Gerri C, Nolte H, Hölper S, Krüger M, Stainier DYR (2015). Genetic compensation induced by deleterious mutations but not gene knockdowns. Nature 524, 230–233.

Schmidt N, Akaaboune M, Gajendran N, Martinez-Pena y Valenzuela I, Wakefield S, Thurnheer R, Brenner HR (2011). Neuregulin/ErbB regulate neuromuscular junction development by phosphorylation of α-dystrobrevin. J Cell Biol 195, 1171–1184.

Schwartz PA, Kuzmic P, Solowiej J, Bergqvist S, Bolanos B, Almaden C, Nagata A, Ryan K, Feng J, Dalvie D, *et al.* (2014). Covalent EGFR inhibitor analysis reveals importance of reversible interactions to potency and mechanisms of drug resistance. Proc Natl Acad Sci USA 111, 173–178.

Stein RA, Staros JV (2000). Evolutionary analysis of the ErbB receptor and ligand families. J Mol Evol 50, 397–412.

Takahashi Y, Fukuda Y, Yoshimura J, Toyoda A, Kurppa K, Moritoyo H, Belzil VV, Dion PA, Higasa K, Doi K, *et al.* (2013). ERBB4 mutations that disrupt the neuregulin-ErbB4 pathway cause amyotrophic lateral sclerosis type 19. Am J Hum Genet 93, 900–905.

Trapnell C, Williams BA, Pertea G, Mortazavi A, Kwan G, Van Baren MJ, Salzberg SL, Wold BJ, Pachter L (2010). Transcript assembly and quantification by RNA-Seq reveals unannotated transcripts and isoform switching during cell differentiation. Nat Biotechnol 28, 511–515.

Trinidad JC, Fischbach GD, Cohen JB (2000). The Agrin/MuSK signaling pathway is spatially segregated from the neuregulin/ErbB receptor signaling pathway at the neuromuscular junction. J Neurosci 20, 8762–8770.

Veldman MB, Lin S (2008). Zebrafish as a developmental model organism for pediatric research. Pediatr Res 64, 470–476.

Williams CC, Allison JG, Vidal GA, Burow ME, Beckman BS, Marrero L, Jones FE (2004). The ERBB4/HER4 receptor tyrosine kinase regulates gene expression by functioning as a STAT5A nuclear chaperone. J Cell Biol 167, 469–478.

Wu YL, Cheng Y, Zhou X, Lee KH, Nakagawa K, Niho S, Tsuji F, Linke R, Rosell R, Corral J, *et al.* (2017). Dacomitinib versus gefitinib as first-line treatment for patients with EGFR-mutation-positive non-small-cell lung cancer (ARCHER 1050): a randomised, open-label, phase 3 trial. Lancet Oncol 18, 1454–1466.

Yang JC, Shih JY, Su WC, Hsia TC, Tsai CM, Ou SH, Yu CJ, Chang GC, Ho CL, Sequist LV, *et al.* (2012). Afatinib for patients with lung adenocarcinoma and epidermal growth factor receptor mutations (LUX-Lung 2): a phase 2 trial. Lancet Oncol 13, 539–548.

Zhu X, Lai C, Thomas S, Burden SJ (1995). Neuregulin receptors, erbB3 and erbB4, are localized at neuromuscular synapses. EMBO J 14, 5842–5848.

Zwaan CM, Kearns P, Caron H, Verschuur A, Riccardi R, Boos J, Doz F, Geoerger B, Morland B, Vassal G (2010). The role of the "innovative therapies for children with cancer" (ITCC) European consortium. Cancer Treat Rev 36, 328–334.